

Alternative $\nu + \nu$ -picture of bosonic fractional Chern insulators at high filling factors in multiple flat-band systems

Licheng Wang,¹ Dong-Hao Guan,¹ Ai-Lei He,^{2,*} Shun-Li Yu,^{1,3,†} and Yuan Zhou^{1,3,‡}

¹*National Laboratory of Solid State Microstructure,*

Department of Physics, Nanjing University, Nanjing 210093, China

²*College of Physics Science and Technology, Yangzhou University, Yangzhou 225002, China*

³*Jiangsu Key Laboratory of Quantum Information Science and Technology, Nanjing University, Nanjing 210093, China*

(Dated: January 21, 2026)

Most fractional quantum Hall states have been traditionally identified within a single energy band, such as the lowest Landau level or topological flat band. As more particles are introduced, they inevitably populate higher energy bands. Whether the inclusion of multiple topological bands leads to new physics remains an open question. Here, we propose a universal picture applicable at higher filling factors $\nu \geq 1$ in bosonic systems: the occupied bands tend to coalesce into an effective single topological band characterized by a total Chern number $|C|$, the sum of the Chern number of all occupied lower topological flat bands. Using a Kekulé lattice model with two lower flat bands featuring a total Chern number $C = 1$, regardless of their specific configurations, we identify the emergence of a $\frac{1}{2}$ fractional Chern insulator (FCI) state at integer filling factor $\nu = 1$, followed by the Jain sequence states $\frac{2}{3}$ and $\frac{3}{4}$ at filling $\nu = \frac{4}{3}$ and $\frac{6}{4}$. That is a $\nu + \nu$ picture, rather than the generally expected $1 + \nu'$ picture, where ν' is the permitted FCI filling factor in the single second topological flat band. Our findings deepen the understanding of FCI states and open avenues for discovering exotic fractional topological phases in multiband systems.

Introduction— The emergence of topological state which beyond Landau’s paradigm has attracted great attentions and become a focal point of research in condensed matter physics over the past two decades [1]. The fractional quantum Hall effect, a the representative of topologically ordered states, was first observed in two-dimensional electronic gas system with partially filled Landau level [2]. Its topological order is characterized by ground states with long-range topological entanglement and quasiparticle with fractional charges [1, 3–6]. The Laughlin’s trial wave function successfully explained the $\nu = \frac{1}{m}$ fractional quantum Hall effect [7]. Jain proposed the new fractional quantum Hall states with the sequence $\nu = \frac{p}{2mp \pm 1}$ for integer p , naturally generalized the Laughlin’s states through the composite-fermion approach [8]. Furthermore, wave functions hosting non-Abelian statistics, such as the Read-Rezayi Z_k parafermion states, were established, enriching the family of fractional quantum Hall states [9–11]. The fractional Chern insulator (FCI) state [12–21], a lattice version of fractional quantum Hall effect in the absence of an external magnetic field, was subsequently proposed in topological flat band (TFB) systems [22–24], and has recently been observed in rhombohedral multilayer graphene and twisted bilayer transition metal dichalcogenides [25–29].

To date, most studies on fractional quantum Hall states have concentrated on the partially filled lowest single band at low filling, either in the Landau level or TFB. This is typically achieved by identifying the bands with

large energy gaps or employing projection Hamiltonians that neglect level mixing effect from higher bands. Potential non-Abelian states were reported at higher filling factors, such as the Pfaffian $\nu = \frac{5}{2}$ state [9, 30], the parafermion $\nu = \frac{12}{5}$ state [31], and the recently proposed $\nu = \frac{3}{2}$ state in twisted bilayer MoTe₂ [32, 33]. Nevertheless, the main physics of these states still originates from a single band (the second topological band) with fully occupied the lowest band, i.e., a $1 + \nu'$ FCI picture with ν' the allowed FCI filling factor on the single higher Landau level or TFB. In fact, the TFB systems can host the multiband characteristic, such as the recently reported second moiré flat band in twisted bilayer MoTe₂ [34, 35]. At higher filling factors, the loaded particles inevitably occupy the multiple bands. This raises the fundamental questions: *Can the proposed FCI states on a single TFB be observed in real system including multiple bands, and will the inclusion of multiple bands introduce new physics beyond the single-band picture?* Indeed, a recently numerical study on moiré FCIs in rhombohedral graphene showed that the $\nu = \frac{1}{3}$ FCI observed in one-band exact diagonalization (ED) algorithm collapses due to band mixing [36].

In this paper, we employ real-space ED without any projection and the infinite density matrix renormalization group (iDMRG) algorithm to explore exotic FCI states of hard-core bosons at higher filling $\nu \geq 1$ on Kekulé lattice model with two lower TFBs. We numerically identify a universal $\frac{1}{2}$ FCI state emerging at $\nu = 1$ when the two lower TFBs collectively contribute a total Chern number $|C_{\text{tot}}| = 1$, regardless of the topological details of the constituent bands, even when including topological trivial bands. The subsequent $\frac{2}{3}$ and $\frac{3}{4}$ Jain sequence states at filling $\nu = \frac{4}{3}$ and $\nu = \frac{6}{4}$ are also

* healei@yzu.edu.cn

† slyu@nju.edu.cn

‡ zhouyuan@nju.edu.cn

verified. Those findings demonstrate a distinct picture in bosonic multi-TFB models at high filling $\nu \geq 1$: the lower TFBs tend to coalesce into an effective single topological band, rather than the generally expected $1 + \nu'$ picture on higher TFB. Our results offer a flexible approach to search FCI states in multiband systems.

Model and methods—We construct a honeycomb lattice with Kekulé-like hopping terms [37–39], with six atomic orbitals per unit cell. We consider the first nearest-neighbor(NN1), the second nearest-neighbor(NN2) and the third nearest-neighbor (NN3) hopping terms with staggered fluxes introduced selectively on some of hopping terms. Within the Kekulé lattice model[Fig 1(a)], the hopping terms are classified into two categories, analogous to the intra- and inter-cell hoppings. We introduce staggered fluxes on the NN1 and NN2 hopping terms, while preserving the sixfold rotational symmetry of the system. Consequently, multifold staggered fluxes enable the realization of multiple topological flat bands with distinct Chern number combinations within the Kekulé lattice model, establishing an ideal platform for searching possible FCI states beyond single band restriction at higher filling.

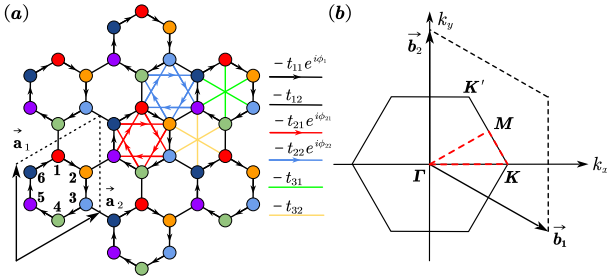


FIG. 1. (a) Schematic structure of the Kekulé lattice model. \vec{a}_1 and \vec{a}_2 are lattice vectors, and the six atomic orbitals in the unit cell (dotted rhombus) are labeled from “1” to “6”. Various hopping terms are illustrated by lines with distinct colors (arrows indicate staggered fluxes), and the right panel displays the associated hopping terms. (b) The first Brillouin zone of the Kekulé lattice. The high-symmetry path Γ - K - M - Γ are marked by red dash line.

The noninteracting Hamiltonian is written as

$$H_0 = -t_{11} \sum_{\langle ij \rangle} e^{i\phi_1} b_i^\dagger b_j - t_{12} \sum_{\langle ij \rangle} b_i^\dagger b_j - t_{21} \sum_{\langle\langle ij \rangle\rangle} e^{i\phi_{21}} b_i^\dagger b_j - t_{22} \sum_{\langle\langle ij \rangle\rangle} e^{i\phi_{22}} b_i^\dagger b_j - t_{31} \sum_{\langle\langle\langle ij \rangle\rangle\rangle} b_i^\dagger b_j - t_{32} \sum_{\langle\langle\langle ij \rangle\rangle\rangle\rangle} b_i^\dagger b_j + \text{H.c.} \quad (1)$$

Here t_{11} and t_{12} denote the intra- and inter-cell hopping amplitudes for NN1, t_{21} and t_{22} for NN2, and t_{31} and t_{32} for NN3, respectively. The staggered phase factors ϕ_1 (on NN1 bonds) , ϕ_{21} and ϕ_{22} (on NN2 bonds) are engineered to generate the TFBs. The operator $b_i^\dagger(b_i)$

creates (annihilates) a hard-core boson at the i th site. To stabilize the FCI states, we introduce hard-core bosons with short-range repulsive interactions, The interaction Hamiltonian is given by

$$H_I = V_1 \sum_{\langle ij \rangle} n_i n_j, \quad (2)$$

with $n_i = b_i^\dagger b_i$ representing the number operator of hard-core bosons at the site i , and V_1 denoting the NN1 repulsion strength.

We employ ED and iDMRG methods to investigate the topological states and topological orders in this model. In ED calculations, we consider a finite system of $N_x \times N_y$ unit cells (total number of sites $N_s = 6 \times N_x \times N_y$), and periodic boundary conditions have been considered. We denote the boson numbers as N_B , and the filling factor of the flat band is $\nu = N_B/(N_x \times N_y)$. The momentum vector $\mathbf{q} = (2\pi k_1/N_1, 2\pi k_2/N_2)$ is labeled as (k_1, k_2) . To study the topological state at larger scales and obtain additional numerical evidence beyond the ED limitations, we also employ the iDMRG algorithm on an $L_x \times L_y$ cylinder geometry with infinite length $L_x \rightarrow \infty$ and finite circumference L_y [40–43].

Multiple low energy flat bands in Kekulé lattice— The bulk energy spectrum is obtained by numerical diagonalization of the Hamiltonian H_0 Eq. (1) following the Fourier transformation. The Chern number of the n th band is defined as $C_n = \frac{1}{2\pi} \int_{\text{BZ}} d^2\mathbf{k} \mathcal{F}_n(\mathbf{k})$, where $\mathcal{F}_n(\mathbf{k}) = \nabla \times \mathcal{A}_n(\mathbf{k})$ is the Berry curvature, while $\mathcal{A}_n(\mathbf{k})$ denoting the Berry connection. The flatness ratio f_n of the n th band is defined as $f_n = \Delta_n/W_n$, where Δ_n denotes the band gap between the n th and the $(n+1)$ th bands, and W_n represents the bandwidth. We explore the parameter space to achieve the multiband exhibiting simultaneously high f_1 and f_2 values.

To generate both high-Chern number and the multiple TFBs, the distant-neighbor hopping terms and multifold staggered fluxes are essential [21, 44, 45]. When including the hopping terms up to the NN2 with staggered fluxes, the parameter space search over $\{t_{11}, t_{12}, t_{21}, t_{22}, \phi_1, \phi_{21}, \phi_{22}\}$ reveals abundant lower double flat bands hosting a total Chern number $|C_{\text{total}}| = 1$. Most of them exhibit Chern numbers $|C_1| = 1$ or 0 for the lowest flat band. Notably, TFBs with a higher Chern number ($C \geq 2$) are rare and host low flatness ratio. We select three representative lower energy double flat bands cases with distinct Chern number combinations, $\{C_1, C_2 = 0, -1\}$, $\{C_1, C_2 = 1, 0\}$ and $\{C_1, C_2 = -1, 2\}$. As shown in Fig 2(a)-(c), the lowest bands host Chern numbers 0, 1 and -1, with the flatness ratios $\{f_1, f_2 = 10.7, 97.2\}$, $\{f_1, f_2 = 5.3, 23.6\}$ and $\{f_1, f_2 = 24.1, 19.6\}$, respectively. To achieve the double flat bands that the lowest band hosts a higher Chern number, we consider the hopping terms up to the NN3 and select a typical double flat bands combination of $\{C_1, C_2 = 2, -1\}$ [Fig 2(d)], and the flatness ratios are $\{f_1, f_2 = 13.5, 25.2\}$.

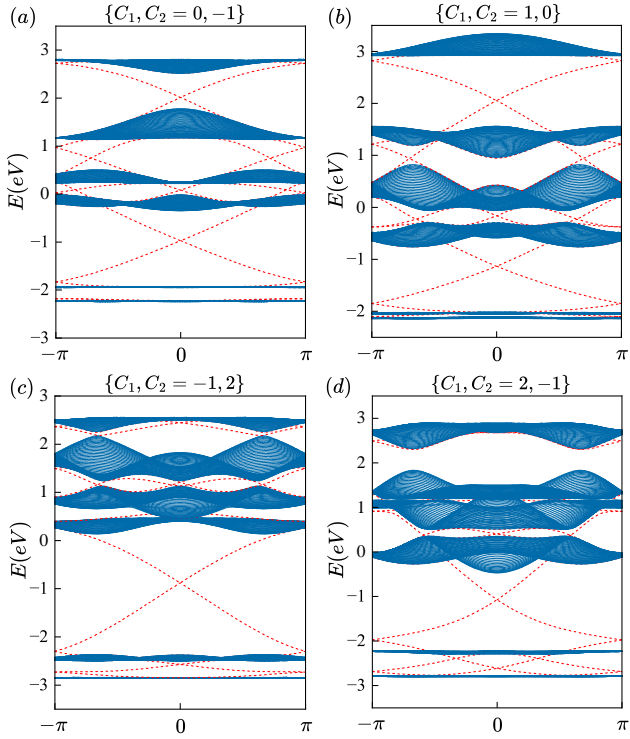


FIG. 2. The energy spectrum of multiband with distinct Chern number combinations on the cylinder geometry, bulk and edge states are represented by blue solid lines and red dashed lines, respectively. (a) multiband with Chern number $\{C_1, C_2\} = \{0, -1\}$. (b) $\{C_1, C_2\} = \{1, 0\}$. (c) $\{C_1, C_2\} = \{-1, 2\}$. (d) $\{C_1, C_2\} = \{2, -1\}$. The detailed parameters are shown Supplementary Materials (SM).

FCI states at lower filling factors $\nu < 1$ —FCI states at low filling factors $\nu < 1$ have been well established on the single TFB in many models, including the bosonic FCIs at $\nu = \frac{r}{r|C|+1}$ and fermionic FCIs at $\nu = \frac{r}{2r|C|+1}$ [12, 13, 17, 18, 46, 47]. We also show the Laughlin-like FCI states on the lowest TFB in SM, including both $\nu = \frac{1}{2}$ FCI state at $|C| = 1$ and $\nu = \frac{1}{3}$ FCI state at $|C| = 2$. Our results confirm the realization of FCI states on the lowest single TFB.

$\frac{1}{2}$ FCI state at integer filling $\nu = 1$ —We start from the integer filling $\nu = 1$ at the situation $\{C_1, C_2 = 0, -1\}$. This case features a topological trivial lowest flat band ($C_1 = 0$), which usually does not support a FCI state with the single-band picture, and thus provide an ideal platform to check the role of multiple TFBs. The low energy spectra of two lattice sizes $N_s = 36$ and 48 with $V_1 = 8.0$ at filling $\nu = 1$ [Fig. 3(a)] exhibit two quasi-degenerate ground states at $(k_x, k_y) = (0, 0)$ in both sizes. For $N_s = 36$, each ground state evolves adiabatically into itself and maintain a robust energy gap from the low excited states under the twist boundary conditions [Fig. 3(b)]. The many-body Chern number of ground states is defined by $C = \frac{1}{2\pi} \int \int d\theta_x d\theta_y F(\theta_x, \theta_y)$. Here,

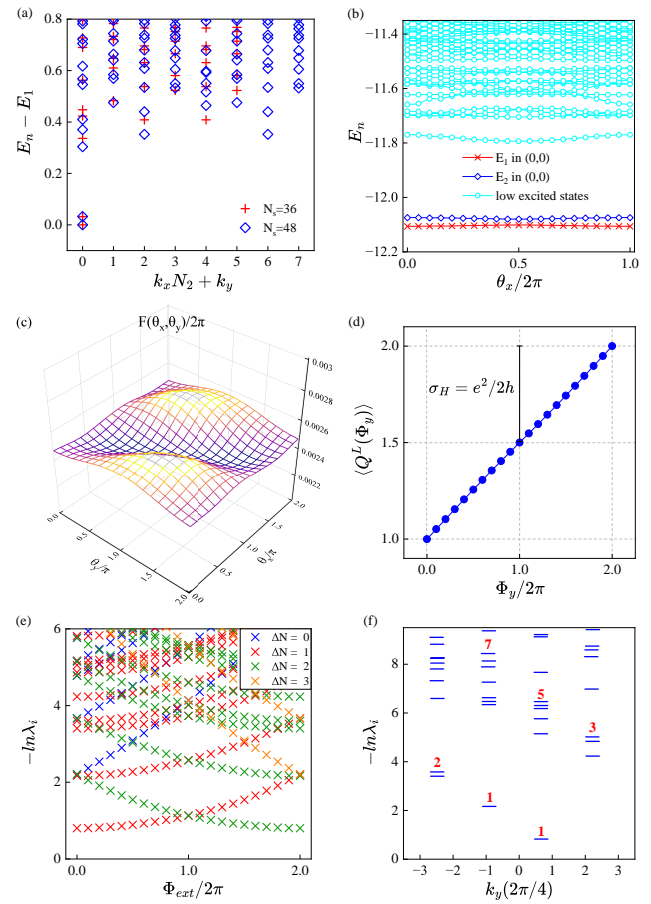


FIG. 3. Topological features at $\nu = 1$ for $\{C_1, C_2\} = \{0, -1\}$ combination. (a) Low-energy spectra with $V_1 = 8.0$ for two lattice sizes $N_s = 6 \times 3 \times 2 = 36$ and $N_s = 6 \times 4 \times 2 = 48$. (b) Low-energy spectrum versus θ_x at a fixed $\theta_y = 0$ in the $N_s = 36$ lattice. (c) Total Berry curvature of the ground states at 20×20 mesh points, indicating a total Chern number $C = 1$. (d) Charge pumping after two flux quanta insertion on a cylinder with $L_y = 4$ and $\chi = 800$. (e) Entanglement spectrum evolution as a function of flux, four charge sectors ΔN are marked by blue, red, green and orange. (f) Momentum-resolved entanglement spectrum on a cylinder with $L_y = 4$ and $\chi = 1800$, revealing one chiral edge mode with counting sequence $(1,1,2,3,5,7,⋯)$.

$F(\theta_x, \theta_y)$ is the many-body Berry curvature $F(\theta_x, \theta_y) = \text{Im}(\langle \frac{\partial \Psi}{\partial \theta_y} | \frac{\partial \Psi}{\partial \theta_x} \rangle - \langle \frac{\partial \Psi}{\partial \theta_x} | \frac{\partial \Psi}{\partial \theta_y} \rangle)$, and Ψ denotes the wave function of the ground state [48]. Numerical results show that each of these two ground states contributes a Chern number of $\frac{1}{2}$, yielding a total many-body Chern number $|C| = 1$. The remarkably smooth Berry curvature of 2π [Fig. 3(c)] confirms that the two ground states collectively yield a total Chern number $|C| = 1$. Furthermore, we obtain the $\langle Q^L(\Phi_y) \rangle$ [Fig. S3(d) in SM] by iDMRG ($\langle Q^L(\Phi_y) \rangle$ is the charge polarization of left half infinite cylinders when flux Φ_y threads the cylinder). It is apparent that the wave function pumps $\frac{1}{2}$ charge after a

flux quanta threading, corresponding to Hall conductivity $\sigma_H \approx 0.5e^2/h$ [49]. We further calculate the entanglement spectrum as a function of flux Φ_y [Fig 3(e)]. The low-lying eigenvalues of the reduced density matrix in charge sectors $\Delta N = 0$ and $\Delta N = 2$ are degenerate at $\Phi_y = 0$. After 2π flux insertion, the symmetry center of spectrum undergoes a shift from $\Delta N = 1$ to $\Delta N = \frac{3}{2}$, corresponding to a net charge transfer of $\frac{1}{2}$ after inserting a flux quantum. The entanglement spectrum under flux insertion exhibits the characteristics of a gapless edge spectrum. At $\Phi_y = 4\pi$, the spectrum becomes symmetric about $\Delta N = 2$. Thus, after inserting two flux quanta, the ground state evolves to itself, which is equivalent to the transfer of two anyons from the left edge to the right edge [42, 50, 51]. Moreover, the momentum-resolved entanglement spectrum indicates one branch of the edge modes with counting sequence $(1, 1, 2, 3, 5, 7, \dots)$, consisting with $\frac{1}{2}$ Laughlin state. These features unambiguously identify the emergent $\frac{1}{2}$ Laughlin FCI state at $\nu = 1$. Considering the fact that the two lower flat bands host $\{C_1, C_2 = 0, -1\}$, our numerical results reveal that the loaded hard-core bosons simultaneously occupy the two lower bands, which coalesce into an effective single topological band with $|C_{\text{tot}}| = 1$. The resultant $\frac{1}{2}$ FCI state at integer filling factor is indeed a $\frac{1}{2} + \frac{1}{2}$ state, which cannot be explained in the framework of single-band picture.

Whether such unexpected FCI state is unique for a specific multi-TFB combination. We further study the more double lower energy TFBs while fixing $|C_{\text{tot}}| = 1$ at $\nu = 1$, including the combinations $\{C_1, C_2 = 1, 0\}$, $\{C_1, C_2 = -1, 2\}$ and $\{C_1, C_2 = 2, -1\}$ as shown in SM. The two quasi-degenerate ground states at fixed momentum point $(k_x, k_y) = (0, 0)$ on torus geometry, the low-energy spectrum and many-body Chern numbers (each ground state contributes $C = \frac{1}{2}$), and $\frac{1}{2}$ charge pumping after one flux quantum insertion on cylinder geometry, as well as the evolution of entanglement spectrum as function of threading flux, well support the emergence of $\frac{1}{2}$ Laughlin FCI at integer filling. Our results thus reveals the intrinsic tendency of hard-core bosons to occupy the effective $|C_{\text{tot}}| = 1$ topological flat band, which consists of two low-energy flat bands, leading to exotic topological states beyond the single-flat-band picture. Such combination of multiple bands to form an effectively single TFB was also observed in recently proposed hyperbolic lattice [52–55], indicating the unique and common properties of multi-band systems in hard-core systems. Similar $\frac{1}{2}$ FCI state at $\nu = 1$ with Chern band combination $\{C_1, C_2 = 2, -1\}$ was previously reported on a specific triangular lattice model [56]. The $\frac{1}{2}$ FCI at $\nu = 1$ with Chern band combination $\{C_1, C_2 = 2, -1\}$ is also in sharp contrast with the numerically proposed bosonic integer quantum Hall state on a generalized Hosftadter lattice with $C = 2$ lowest TFB [57], where the many-body Chern number is 2.

Jain sequence states at $\nu > 1$ —Having established a new $\nu + \nu$ picture in multi-band system: the loaded hard-core bosons favor to occupy two lower TFBs simultane-

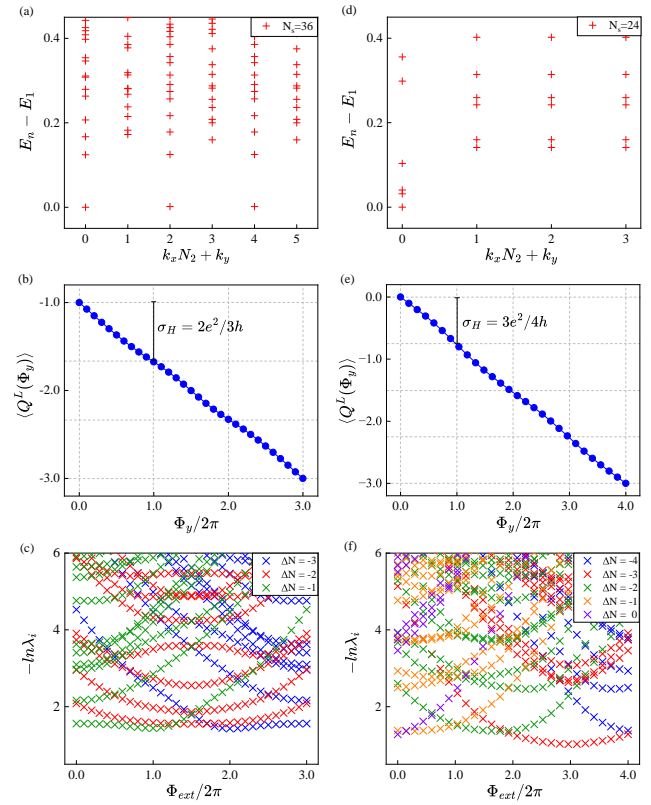


FIG. 4. Topological features at $\nu = \frac{4}{3}$ with $N_s = 6 \times 3 \times 2 = 36$ (left panels) and at $\nu = \frac{6}{4}$ with $N_s = 6 \times 2 \times 2 = 24$ (right panels) for $\{C_1, C_2 = 1, 0\}$ combination. (a) and (d) Low-energy spectrum; (b) and (e) Charge pumping after flux quanta threading on cylinder geometry with $L_y = 3$ and $\chi = 600$ ((b)) and $L_y = 3$ and $\chi = 800$ ((d)); and (c) and (f) Entanglement spectrum evolution as functions of flux insertion.

ously, which generates an effective topological band with $|C_{\text{tot}}| = |C_1 + C_2| = 1$. To verify this picture, we further study the $\nu > 1$ cases, in which the loaded hard-core bosons naturally occupy the higher TFB. Whether more FCI states, e.g., the Jain sequence state can be observed in the present multi-TFB systems.

We choose a multi-TFB system with Chern number combination $\{C_1, C_2 = 1, 0\}$ as example (more in SM). The relatively small band gap between the two flat bands facilitates the realization of hierarchy daughter states [58]. The low-energy spectrum for $N_s = 36$ at $\nu = \frac{4}{3}$ filling reveals three quasi-degenerate ground states, separated from the low excited states by a gap. The charge pumping after the adiabatic insertion of three flux quanta is -2 , perfectly matches the quantized Hall conductances of $\frac{2}{3}$ [Fig. 4(a) and (b)]. The lowest level of entanglement spectrum [Fig. 4(c)] is shifted from $\Delta N = -1$ to $\Delta N = -3$ after inserting three flux quanta, indicating a net charge transfer of 2 from left edge to the right edge, while the ground states evolving to itself. Since

the Chern number of the second TFB is $C_2 = 0$, FCI states are not permitted on the single second TFB band at $\nu = 1 + \frac{1}{2}, 1 + \frac{2}{3}, \dots$ with respective two-, three-fold, \dots ground states degeneracies, where “1” denotes the fully occupied lowest band. The observed $\frac{2}{3}$ FCI state at $\nu = \frac{4}{3}$ thus cannot be contributed by the single second TFB band. In contrast, a first daughter state of $\frac{1}{2}$ on an effective single band $|C| = 1$ well matches all the features of topological order. In SM, we show more numerical evidences for the Jain states at $\nu = \frac{4}{3}$. For $C_2 = 1, 1 + \frac{1}{2}$ (Laughlin-like state, twofold ground state degeneracy with $\nu = \frac{3}{2}$) and $1 + \frac{2}{3}$ (first Jain state, three-fold ground state degeneracy with $\nu = \frac{5}{3}$) are permitted in $1 + \nu'$ picture on the second TFB, and thus do not match the observed topological feature at $\nu = \frac{4}{3}$. Similarly, at $\nu = \frac{3}{2}$ ($\frac{6}{4}$), we observe the four-fold quasi-degenerate ground states in the $(k_x, k_y) = (0, 0)$ sector, 3 charge pumping after adiabatic threading four flux quanta [Fig. 4(d) and (e)]. The inserting four flux quanta shifts the entanglement spectrum [Fig. 4(f)] from $\Delta N = 0$ to $\Delta N = -3$, indicating a net charge transfer of 3 from left edge to the right edge. These topological features manifest the emergent state is a $\frac{3}{4}$ FCI state. Interestingly, the potential $1 + \frac{1}{3}$ Laughlin-like FCI state on the second TFB band for $\{C_1, C_2 = -1, 2\}$ case shares the same similar nature as the first Jain sequence $\frac{2}{3} + \frac{2}{3}$ discussed above. Whether they are exactly the same or distinguishable remains unclear.

We, therefore, identify the general tendency in multi-TFB system—the lower TFBs collectively contribute an effective topological band with $C_{\text{tot}} = \sum_{i \in \text{occ}} C_i$ —at high filling factors $\nu \geq 1$. These emergent FCI states show clear differences from the commonly expected $1 + \nu'$ FCI states in higher TFB. In general, the emergence of FCI requires TFB with high flatness ratio in single TFB systems. It is quite amazing that the robust FCI states can be established at the condition with low flatness, e.g., the flatness ratio of the effective single topological band is as low as $f_{\text{tot}} \sim 4$ (SM). Our results provide new opportunity to search robust FCI states in multi-band system with more flexible requirements, even for the condition of trivial topology.

Conclusion and discussions—We reveal a universal picture in strongly correlated multi-TFB systems at high fillings $\nu \geq 1$: the lower TFBs coalesce into an effec-

tive topological band, with its Chern number being the sum of the Chern numbers of the occupied lower bands, irrespective of their specific configurations. Based on a Kekulé lattice model with two lower TFBs and a total Chern number $|C_{\text{tot}}| = 1$, we numerically identify that the emergence of the $\frac{1}{2}$ -Laughlin-like bosonic FCI at integer filling $\nu = 1$, as well as the subsequent $\frac{2}{3}$ and $\frac{3}{4}$ Jain state at higher filling $\nu = \frac{4}{3}$ and $\nu = \frac{3}{2}$ ($\frac{6}{4}$). Those $\nu + \nu'$ FCI states on multi-TFB system break the widely expected $1 + \nu'$ -picture on higher TFB. Our findings highlight the essential difference of fractional quantum Hall states between the single- and multi-TFB system, and reveal unique FCIs which cannot be achieved via single-band projection method.

So far, only bosonic FCI states on the effective $|C| = 1$ condition is well established. Whether the bosonic FCI states can be realized on the effective single bands with higher Chern number, as well as the fermionic counterparts, remain unknown. Moreover, since the hard-core bosons with higher filling factors tend to occupy the multiple bands, whether two distinct FCI states, each of which is realized in the respective TFBs, will emerge under suitable conditions is quite interesting. Systems with multiple TFBs provide the possibility for the realization of such composite FCI states, is an interesting problem that deserves further study. In addition, recently theoretical studies proposed the Moore-Read Pfaffian states in twist transition metal dichalcogenides [33, 59, 60]. The single-particle band structure of this system hosts three moiré flat bands with unit Chern numbers 1, forming a multiband system. The interplay between multiband occupation and particles with more complex interactions, may yield some novel non-Abelian FCI states. The relative looser condition for the FCI state observed in multiband system may provide alternative access for the non-Abelian states.

Acknowledgement—This work was supported by the National Natural Science Foundation of China (Grants No. 12204404 No. 12374137, and No. 12434005) and the Natural Science Foundation of Jiangsu Province (Grant No. BK20231397).

Data availability—The data that support the findings of this article are not publicly available. The data are available from the authors upon reasonable request.

[1] X. G. WEN, Topological orders in rigid states, *Int. J. Mod. Phys. B* **04**, 239 (1990).

[2] D. C. Tsui, H. L. Stormer, and A. C. Gossard, Two-dimensional magnetotransport in the extreme quantum limit, *Phys. Rev. Lett.* **48**, 1559 (1982).

[3] F. D. M. Haldane, “fractional statistics” in arbitrary dimensions: A generalization of the pauli principle, *Phys. Rev. Lett.* **67**, 937 (1991).

[4] X.-G. Wen, Topological orders and edge excitations in fractional quantum hall states, *Adv. Phys.* **44**, 405 (1995).

[5] A. Kitaev and J. Preskill, Topological entanglement entropy, *Phys. Rev. Lett.* **96**, 110404 (2006).

[6] M. Levin and X.-G. Wen, Detecting topological order in a ground state wave function, *Phys. Rev. Lett.* **96**, 110405 (2006).

[7] R. B. Laughlin, Anomalous quantum hall effect: An incompressible quantum fluid with fractionally charged ex-

citations, *Phys. Rev. Lett.* **50**, 1395 (1983).

[8] J. K. Jain, Composite-fermion approach for the fractional quantum hall effect, *Phys. Rev. Lett.* **63**, 199 (1989).

[9] G. Moore and N. Read, Nonabelions in the fractional quantum hall effect, *Nucl. Phys. B* **360**, 362 (1991).

[10] N. Read and E. Rezayi, Quasiholes and fermionic zero modes of paired fractional quantum hall states: The mechanism for non-abelian statistics, *Phys. Rev. B* **54**, 16864 (1996).

[11] N. Read and D. Green, Paired states of fermions in two dimensions with breaking of parity and time-reversal symmetries and the fractional quantum hall effect, *Phys. Rev. B* **61**, 10267 (2000).

[12] D. N. Sheng, Z.-C. Gu, K. Sun, and L. Sheng, Fractional quantum hall effect in the absence of landau levels, *Nat. Commun.* **2**, 389 (2011), article.

[13] Y.-F. Wang, Z.-C. Gu, C.-D. Gong, and D. N. Sheng, Fractional quantum hall effect of hard-core bosons in topological flat bands, *Phys. Rev. Lett.* **107**, 146803 (2011).

[14] N. Regnault and B. A. Bernevig, Fractional chern insulator, *Phys. Rev. X* **1**, 021014 (2011).

[15] X.-L. Qi, Generic wave-function description of fractional quantum anomalous hall states and fractional topological insulators, *Phys. Rev. Lett.* **107**, 126803 (2011).

[16] Y.-F. Wang, H. Yao, Z.-C. Gu, C.-D. Gong, and D. N. Sheng, Non-abelian quantum hall effect in topological flat bands, *Phys. Rev. Lett.* **108**, 126805 (2012).

[17] G. Möller and N. R. Cooper, Fractional chern insulators in harper-hofstadter bands with higher chern number, *Phys. Rev. Lett.* **115**, 126401 (2015).

[18] Z. Liu, E. J. Bergholtz, H. Fan, and A. M. Läuchli, Fractional chern insulators in topological flat bands with higher chern number, *Phys. Rev. Lett.* **109**, 186805 (2012).

[19] A. Sterdyniak, C. Repellin, B. A. Bernevig, and N. Regnault, Series of abelian and non-abelian states in $C > 1$ fractional chern insulators, *Phys. Rev. B* **87**, 205137 (2013).

[20] A. M. Läuchli, Z. Liu, E. J. Bergholtz, and R. Moessner, Hierarchy of fractional chern insulators and competing compressible states, *Phys. Rev. Lett.* **111**, 126802 (2013).

[21] Z.-Y. Lan, A.-L. He, and Y.-F. Wang, Flat bands with high chern numbers and multiple flat bands in multifold staggered-flux models, *Phys. Rev. B* **107**, 235116 (2023).

[22] E. Tang, J.-W. Mei, and X.-G. Wen, High-temperature fractional quantum hall states, *Phys. Rev. Lett.* **106**, 236802 (2011).

[23] K. Sun, Z. Gu, H. Katsura, and S. Das Sarma, Nearly flatbands with nontrivial topology, *Phys. Rev. Lett.* **106**, 236803 (2011).

[24] T. Neupert, L. Santos, C. Chamon, and C. Mudry, Fractional quantum hall states at zero magnetic field, *Phys. Rev. Lett.* **106**, 236804 (2011).

[25] J. Cai, E. Anderson, C. Wang, X. Zhang, X. Liu, W. Holtzmann, Y. Zhang, F. Fan, T. Taniguchi, K. Watanabe, Y. Ran, T. Cao, L. Fu, D. Xiao, W. Yao, and X. Xu, Signatures of fractional quantum anomalous Hall states in twisted MoTe₂, *Nature* **622**, 63 (2023).

[26] Y. Zeng, Z. Xia, K. Kang, J. Zhu, P. Knüppel, C. Vaswani, K. Watanabe, T. Taniguchi, K. F. Mak, and J. Shan, Thermodynamic evidence of fractional Chern insulator in moiré MoTe₂, *Nature* **622**, 69 (2023).

[27] H. Park, J. Cai, E. Anderson, Y. Zhang, J. Zhu, X. Liu, C. Wang, W. Holtzmann, C. Hu, Z. Liu, T. Taniguchi, K. Watanabe, J.-H. Chu, T. Cao, L. Fu, W. Yao, C.-Z. Chang, D. Cobden, D. Xiao, and X. Xu, Observation of fractionally quantized anomalous Hall effect, *Nature* **622**, 74 (2023).

[28] F. Xu, Z. Sun, T. Jia, C. Liu, C. Xu, C. Li, Y. Gu, K. Watanabe, T. Taniguchi, B. Tong, J. Jia, Z. Shi, S. Jiang, Y. Zhang, X. Liu, and T. Li, Observation of Integer and Fractional Quantum Anomalous Hall Effects in Twisted Bilayer MoTe₂, *Phys. Rev. X* **13**, 031037 (2023).

[29] Z. Lu, T. Han, Y. Yao, A. P. Reddy, J. Yang, J. Seo, K. Watanabe, T. Taniguchi, L. Fu, and L. Ju, Fractional quantum anomalous Hall effect in multilayer graphene, *Nature* **626**, 759 (2024).

[30] R. Willett, J. P. Eisenstein, H. L. Störmer, D. C. Tsui, A. C. Gossard, and J. H. English, Observation of an even-denominator quantum number in the fractional quantum hall effect, *Phys. Rev. Lett.* **59**, 1776 (1987).

[31] J. S. Xia, W. Pan, C. L. Vicente, E. D. Adams, N. S. Sullivan, H. L. Störmer, D. C. Tsui, L. N. Pfeiffer, K. W. Baldwin, and K. W. West, Electron correlation in the second landau level: A competition between many nearly degenerate quantum phases, *Phys. Rev. Lett.* **93**, 176809 (2004).

[32] K. Kang, B. Shen, Y. Qiu, Y. Zeng, Z. Xia, K. Watanabe, T. Taniguchi, J. Shan, and K. F. Mak, Evidence of the fractional quantum spin hall effect in moiré MoTe₂, *Nature* **628**, 522 (2024).

[33] F. Chen, W.-W. Luo, W. Zhu, and N. S. D, Robust non-Abelian even-denominator fractional Chern insulator in twisted bilayer MoTe₂, *Nat. Commun.* **16**, 2115 (2025).

[34] H. Park, J. Cai, E. Anderson, X.-W. Zhang, X. Liu, W. Holtzmann, W. Li, C. Wang, C. Hu, Y. Zhao, T. Taniguchi, K. Watanabe, J. Yang, D. Cobden, J.-h. Chu, N. Regnault, A. B. B. L. Fu, T. Cao, D. Xiao, and X. Xu, Ferromagnetism and topology of the higher flat band in a fractional chern insulator, *Nature Physics* **21**, 549 (2025).

[35] F. Xu, X. Chang, J. Xiao, Y. Zhang, F. Liu, Z. Sun, N. Mao, N. Peshcherenko, J. Li, K. Watanabe, T. Taniguchi, B. Tong, L. Lu, J. Jia, D. Qian, Z. Shi, Y. Zhang, X. Liu, S. Jiang, and T. Li, Interplay between topology and correlations in the second moiré band of twisted bilayer MoTe₂, *Nature Physics* **21**, 542 (2025).

[36] J. Yu, J. Herzog-Arbeitman, Y. H. Kwan, N. Regnault, and B. A. Bernevig, Moiré fractional chern insulators. iv. fluctuation-driven collapse in multiband exact diagonalization calculations on rhombohedral graphene, *Phys. Rev. B* **112**, 075110 (2025).

[37] T. Kariyado and X. Hu, Topological States Characterized by Mirror Winding Numbers in Graphene with Bond Modulation, *Sci. Rep.* **7**, 16515 (2017).

[38] F. Liu, M. Yamamoto, and K. Wakabayashi, Topological edge states of honeycomb lattices with zero berry curvature, *J. Phys. Soc. Jpn* **86**, 123707 (2017).

[39] L.-H. Wu and X. Hu, Scheme for achieving a topological photonic crystal by using dielectric material, *Phys. Rev. Lett.* **114**, 223901 (2015).

[40] S. R. White, Density matrix formulation for quantum renormalization groups, *Phys. Rev. Lett.* **69**, 2863 (1992).

[41] I. P. McCulloch, *Infinite size density matrix renormalization group, revisited* (2008), arXiv:0804.2509.

[42] A. G. Grushin, J. Motruk, M. P. Zaletel, and F. Pollmann, Characterization and stability of a fermionic $\nu =$

1/3 fractional chern insulator, *Phys. Rev. B* **91**, 035136 (2015).

[43] L. Cincio and G. Vidal, Characterizing topological order by studying the ground states on an infinite cylinder, *Phys. Rev. Lett.* **110**, 067208 (2013).

[44] E. Kapit and E. Mueller, Exact parent hamiltonian for the quantum hall states in a lattice, *Phys. Rev. Lett.* **105**, 215303 (2010).

[45] D. Sticlet and F. Piéchon, Distant-neighbor hopping in graphene and haldane models, *Phys. Rev. B* **87**, 115402 (2013).

[46] A. G. Grushin, T. Neupert, C. Chamon, and C. Mudry, Enhancing the stability of a fractional chern insulator against competing phases, *Phys. Rev. B* **86**, 205125 (2012).

[47] D. Wang, Z. Liu, J. Cao, and H. Fan, Tunable band topology reflected by fractional quantum hall states in two-dimensional lattices, *Phys. Rev. Lett.* **111**, 186804 (2013).

[48] D. N. Sheng, X. Wan, E. H. Rezayi, K. Yang, R. N. Bhatt, and F. D. M. Haldane, Disorder-driven collapse of the mobility gap and transition to an insulator in the fractional quantum hall effect, *Phys. Rev. Lett.* **90**, 256802 (2003).

[49] W.-W. Luo, A.-L. He, Y. Zhou, Y.-F. Wang, and C.-D. Gong, Quantum phase transitions in a $\nu = \frac{1}{2}$ bosonic fractional chern insulator, *Phys. Rev. B* **102**, 155120 (2020).

[50] W. Zhu, S. S. Gong, F. D. M. Haldane, and D. N. Sheng, Topological characterization of the non-abelian moore-read state using density-matrix renormalization group, *Phys. Rev. B* **92**, 165106 (2015).

[51] W. Zhu, S. S. Gong, and D. N. Sheng, Chiral and critical spin liquids in a spin- $\frac{1}{2}$ kagome antiferromagnet, *Phys. Rev. B* **92**, 014424 (2015).

[52] H. Yuan, W. Zhang, Q. Pei, and X. Zhang, Hyperbolic topological flat bands, *Phys. Rev. B* **109**, L041109 (2024).

[53] A.-L. He, L. Qi, Y. Liu, and Y.-F. Wang, Hyperbolic fractional chern insulators, *Phys. Rev. B* **110**, 195113 (2024).

[54] D.-H. Guan, L. Qi, Y. Zhou, A.-L. He, and Y.-F. Wang, Topological flat bands in hyperbolic lattices, *Phys. Rev. B* **111**, 165144 (2025).

[55] D.-H. Guan, Y. Zhou, A.-L. He, and Y.-F. Wang, Topological flat bands in hyperbolic haldane models, *Phys. Rev. B* **112**, 205102 (2025).

[56] W.-W. Luo, A.-L. He, Y.-F. Wang, Y. Zhou, and C.-D. Gong, Bosonic fractional chern insulating state at integer fillings in a multiband system, *Phys. Rev. B* **104**, 115126 (2021).

[57] T.-S. Zeng, W. Zhu, and D. N. Sheng, Bosonic integer quantum hall states in topological bands with chern number two, *Phys. Rev. B* **93**, 195121 (2016).

[58] F. D. M. Haldane, Fractional quantization of the hall effect: A hierarchy of incompressible quantum fluid states, *Phys. Rev. Lett.* **51**, 605 (1983).

[59] C.-E. Ahn, W. Lee, K. Yananose, Y. Kim, and G. Y. Cho, Non-abelian fractional quantum anomalous hall states and first landau level physics of the second moiré band of twisted bilayer mote₂, *Phys. Rev. B* **110**, L161109 (2024).

[60] A. P. Reddy, N. Paul, A. Abouelkomsan, and L. Fu, Non-abelian fractionalization in topological minibands, *Phys. Rev. Lett.* **133**, 166503 (2024).